Figure S1. Related to Figure 1.

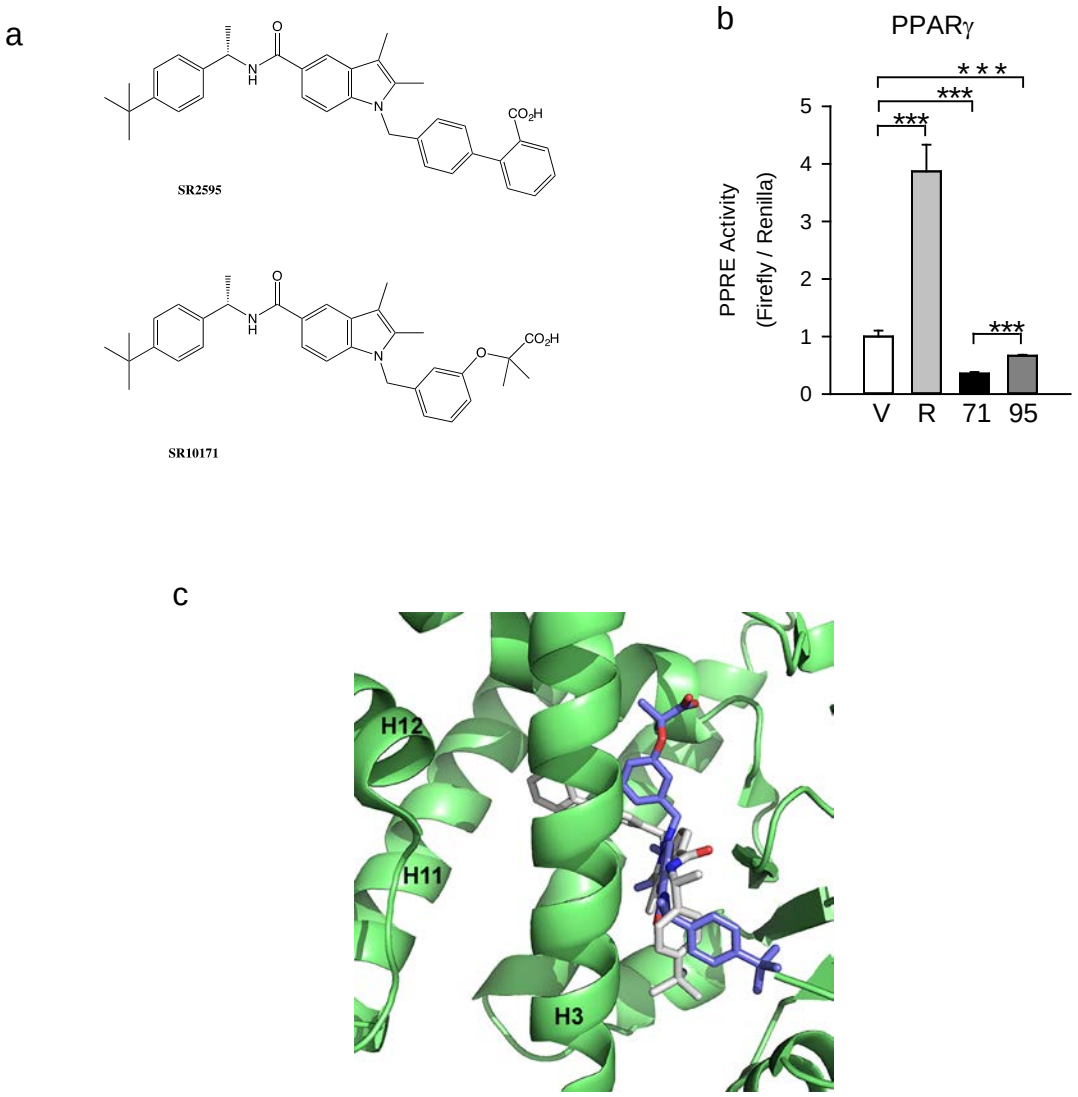

Figure S1. Comparison of SR10171 and SR2595 inverse agonists. (a) Chemical structure of SR2595 and SR10171 compounds. (b) Analysis of PPARγ transcriptional activity in luciferase reporter gene assay. (c) Top scoring in silico docking binding pose for SR10171 (blue) and SR2595 (gray) using chain A of PDB:4R06 (atomic coordinates specific for PPARγ crystal structure from the Protein Structure Database). Data are shown as the mean +/- S.D. Statistical analyses were performed using One Way Anova and significant differences are shown between treated groups and control group. *P < 0.05; **P < 0.01

Figure S1

d

Sequence	Charge	Start	End	Structure	Rosi hsPPARg2 RXR hetero…	SR10171 hsPPARg2 RXR hetero…	SR2595 hsPPARg2 RXR hetero…
LAEISSDIDQLNPESADL		2	222	239	2 (7)*	-1 (5)*	0 (4)*
ISSDIDQLNPESADL		2	225	239	-3 (10)*	-3 (6)*	0 (3)*
IDQLNPESADL		2	229	239	1 (7)*	-2 (5)*	0 (5)*
RALAKHLYDSYIKSFPLTKAKARAIL		4	240	265	-1 (1)*	-9 (1)	1 (2)*
YIKSFPLTKAKARAIL		4	250	265	-2 (6)*	-6 (3)	-2 (3)*
IKSFPLTKAKARAIL		3	251	265	-2 (7)*	-6 (3)	-2 (4)*
IKSFPLTKAKARAIL		4	251	265	-2 (6)*	-6 (3)	-2 (3)*
TGKTTDKSPFVIY		3	266	278	-2 (5)*	0 (4)*	3 (4)*
TGKTTDKSPFVIYDM		2	266	280	1 (4)*	1 (3)*	5 (7)*
TGKTTDKSPFVIYDMNS		3	266	282	3 (6)*	3 (2)*	3 (4)*
DMNSLM		1	279	284	-2 (5)*	-3 (5)*	5 (6)*
MGEDKIKFKHITPLQEQSKEVA		4	285	306	1 (6)*	-3 (5)*	-3 (4)*
IRIFQGCQF		2	307	315	-59 (8)	-45 (5)	-43 (6)
FRSVE		2	315	319	-54 (5)	-51 (5)	-42 (6)
FRSVEA		2	315	320	-49 (4)	-47 (4)	-39 (5)
RSVEAVQE		2	316	323	-21 (5)	-20 (4)	-19 (2)
AVQEITE		1	320	326	-9 (3)	-10 (2)	-4 (2)
AVQEITE		2	320	326	-9 (3)	-9 (2)	-3 (2)
VQEITE		1	321	326	-7 (4)	-7 (3)	-3 (2)
YAKSIPGF		2	327	334	0 (1)*	-1 (1)*	0 (1)*
YAKSIPGFVNL		2	327	337	0 (3)*	-1 (1)*	0 (1)*
YAKSIPGFVNLDL		2	327	339	0 (4)*	-2 (1)*	-1 (2)*
DLNDQVTL		1	338	345	0 (2)*	-2 (1)*	0 (2)*
DLNDQVTLL		2	338	346	-1 (3)*	-2 (2)*	0 (2)*
KYGVHEIIYTML		3	347	358	1 (5)*	0 (5)*	0 (6)*
IIYTML		1	353	358	0 (1)*	0 (1)*	0 (1)*
ASLMNKDGVL		2	359	368	0 (2)*	0 (1)*	0 (1)*
ISEGQGFMTRE		2	369	379	-4 (3)	-8 (3)	-5 (3)
ISEGQGFMTREFL		2	369	381	-3 (4)	-7 (3)	-4 (2)
FLKSLRKPFGDFMEPKFEF		4	380	398	-2 (3)*	-2 (3)*	-2 (3)*
KSLRKPFGDFMEPKFEF		3	382	398	-4 (5)*	3 (5)*	-2 (6)*
LRKPFGDFMEPKFEF		3	384	398	-2 (3)*	-2 (3)*	-2 (3)*
AVKFNA		2	399	404	-3 (6)*	-1 (2)*	-1 (2)*
AVKFNALEL		2	399	407	-2 (5)*	-1 (2)*	0 (2)*
AVKFNALELDDSDL		2	399	412	-1 (4)*	-1 (1)*	0 (1)*
NALELDDSDL		1	403	412	0 (5)*	0 (3)*	0 (2)*
LDDSDL		1	407	412	-2 (8)*	-1 (3)*	0 (3)*
VIILSGDRPGLL		2	418	429	-2 (6)*	-2 (2)*	-1 (3)*
IILSGDRPGL		2	419	428	-3 (6)*	-2 (2)*	-1 (3)*
IILSGDRPGLL		2	419	429	-2 (7)*	-2 (2)*	-1 (3)*
IILSGDRPGLLNVKPIEDIQDNLLQA		3	419	444	-2 (5)*	-2 (1)*	-1 (2)*
NVKPIEDIQDNL		2	430	441	0 (2)*	-1 (1)*	0 (1)*
NVKPIEDIQDNLLQA		2	430	444	0 (2)*	-1 (1)*	0 (1)*
LELQLKLNHPESSQL		2	445	459	0 (5)*	-1 (2)*	0 (2)*
LQLKLNHPESSQL		2	447	459	1 (7)*	-1 (4)*	-2 (3)*
QLKLNHPESSQL		2	448	459	-1 (7)*	-2 (3)*	-1 (3)*
KLNHPESSQL		2	450	459	-1 (9)*	-2 (4)*	-1 (4)*
LQKMTDL		2	464	470	-2 (2)*	-2 (2)*	-4 (3)
LQKMTDLRQ		2	464	472	-4 (2)	-2 (2)*	-4 (3)
LQKMTDLRQ		3	464	472	-4 (2)	-3 (2)*	-4 (3)
LRQIVTE		2	470	476	-17 (4)	-5 (2)	-5 (3)
RQIVTEHVQL		3	471	480	-21 (3)	-4 (3)	-5 (3)
HVQLLQVIKKTETDMSLHPLL		4	477	497	-7 (5)	-5 (3)	-7 (4)
LQVIKKTETDMSLHPLL		2	481	497	-6 (6)	-6 (4)	-6 (5)
LQVIKKTETDMSLHPLL		3	481	497	-6 (6)	-6 (4)	-6 (5)
LQVIKKTETDMSLHPLLQE		3	481	499	-7 (4)	-6 (4)	-6 (5)
SLHPLLQEIYKDLY		3	492	505	-28 (6)	-5 (3)	-7 (4)
QEIYKDLY		2	498	505	-29 (7)	-4 (4)	-5 (4)

Figure S1. Comparison of SR10171 and SR2595 inverse agonists. (d) Alterations in the conformational dynamics of PPARγ upon ligand binding. Perturbation summary view displaying differential hydrogen/deuterium exchange (HDX) data of the ligand-binding domain region of full length PPARγ in the absence (apo receptor) and presence of ligands. HDX was performed on the intact full length RXRα/PPARγ heterodimer in the presence of DMSO only or bound to rosiglitazone, SR10171, and SR2595. Cool colors represent decreased solvent exchange (protection to solvent exchange is indicative of increased stabilization or decreased conformational mobility) and warm colors represent increased solvent exchange (decreased stabilization or increased conformational mobility). Gray color represents regions of the receptor for which no statistically significant change in conformational mobility was observed when comparing apo receptor to liganded receptor.

Figure S1

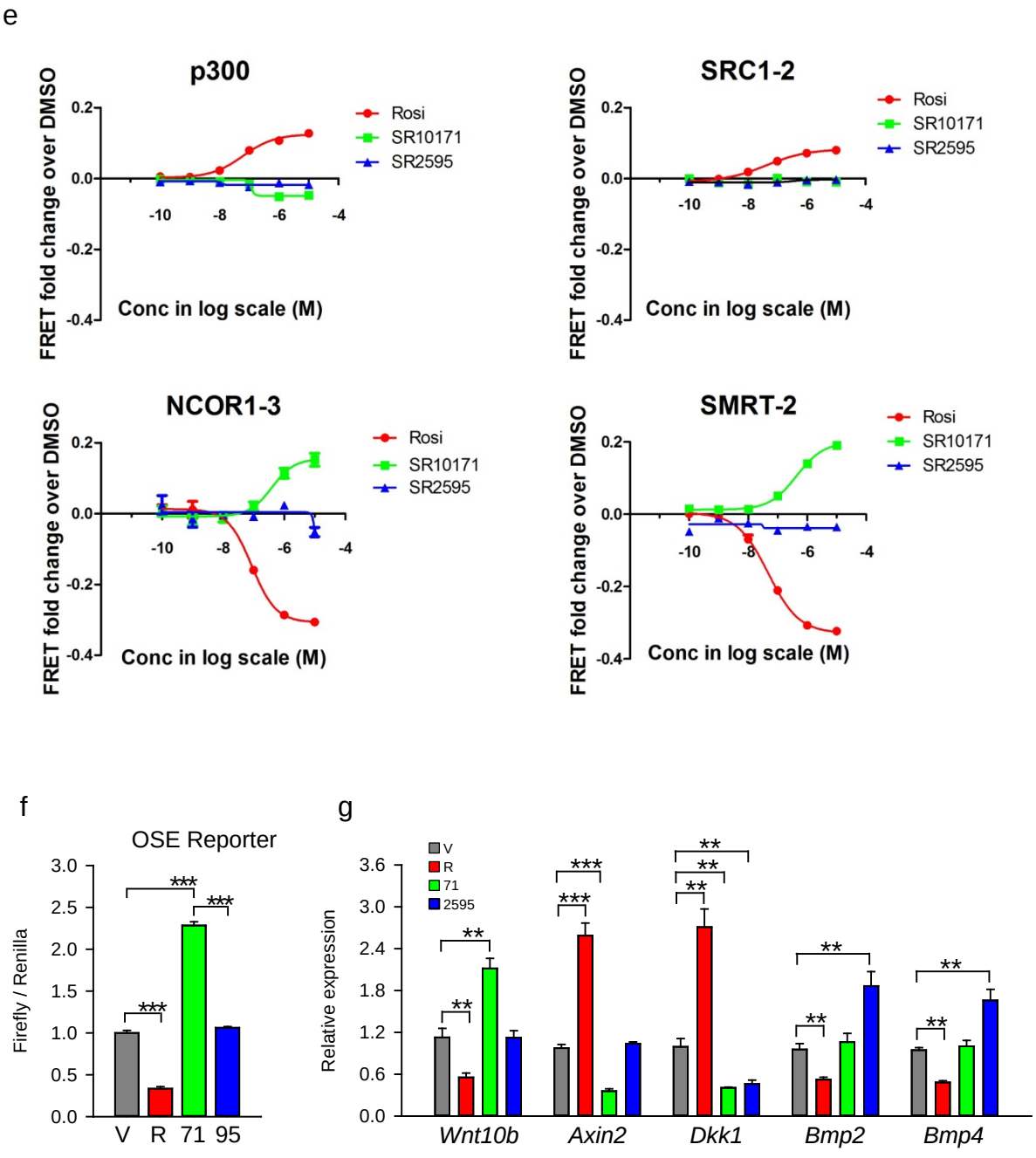

Figure S1. Comparison of SR10171 and SR2595 inverse agonists. (e) TR-FRET analysis of full length His-PPARγ2 interaction with FITC-labeled peptides representative of NR and differential affinity for peptides representative of NR binding motifs from either transcriptional co-activators (p300 and SRC1) or co-repressors (NCOR and SMRT) in the presence of increasing concentrations of SR10171, SR2595, or rosiglitazone. (f) The effect on transcriptional activity of RUNX2 measured in gene reporter assay in U33/γ2 cells transfected with promoter construct 6OSE:luc carrying 6 RUNX2 response elements. (g) The effect on expression of components of Wnt and BMP signaling in primary marrow MSCs treated *ex vivo*, as described in Experimental Procedures. Data are shown as the mean +/- SD. Statistical analyses were performed using One Way Anova and significant differences are shown between treated groups and control group. *P < 0.05; **P < 0.01

Figure S2. Related to Figure 2.

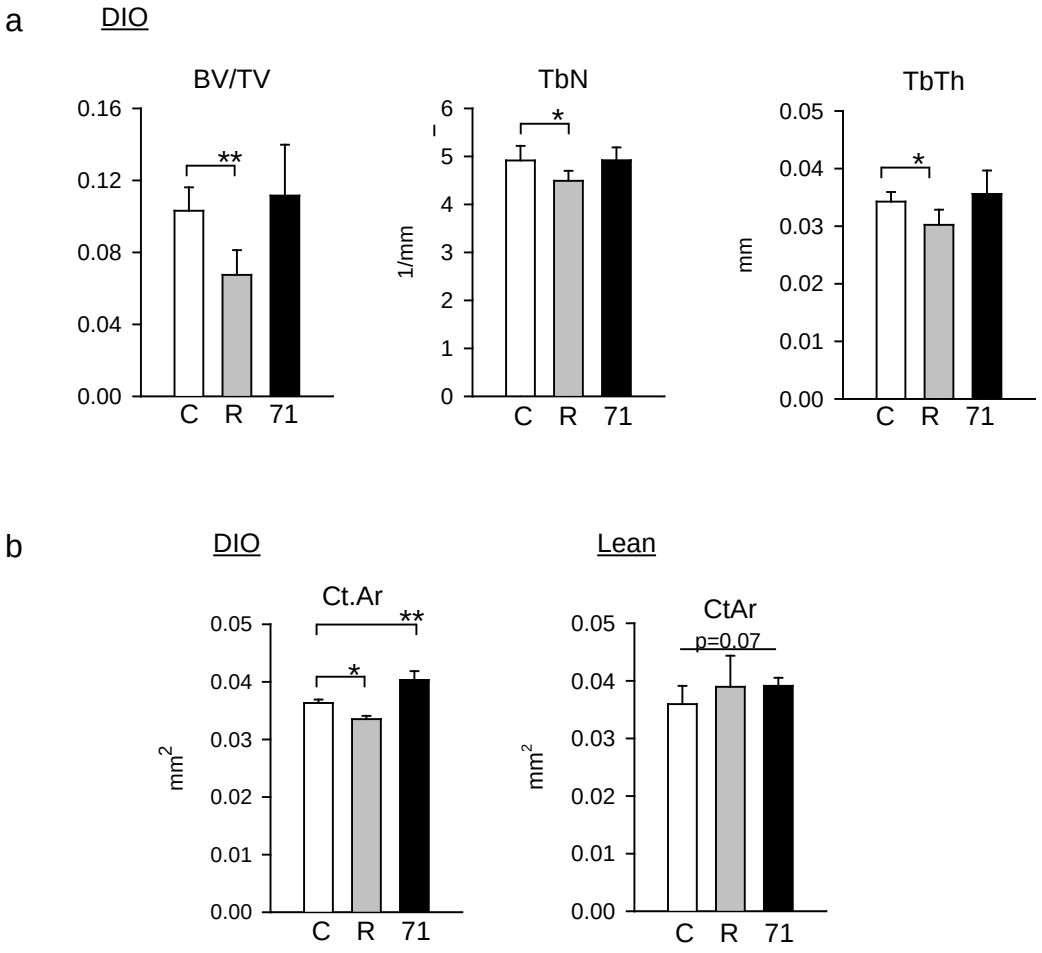

Figure S2. Effect of SR10171 and rosiglitazone on trabecular bone in vertebra (a) and cortical bone in midshaft tibia (b) of DIO and lean animals at the end of experiment (n=8 animals per group). mCT measurements: BV/TV – bone mass; TbN – trabecular number; TbTh- trabecular thickness; Ct.Ar – cortical area; All data are shown as the mean +/- s.d. Statistical analyses were performed using One Way Anova and significant differences are shown between treated groups and control group. *P < 0.05; **P < 0.01.

Figure S3. Related to Figure 2.

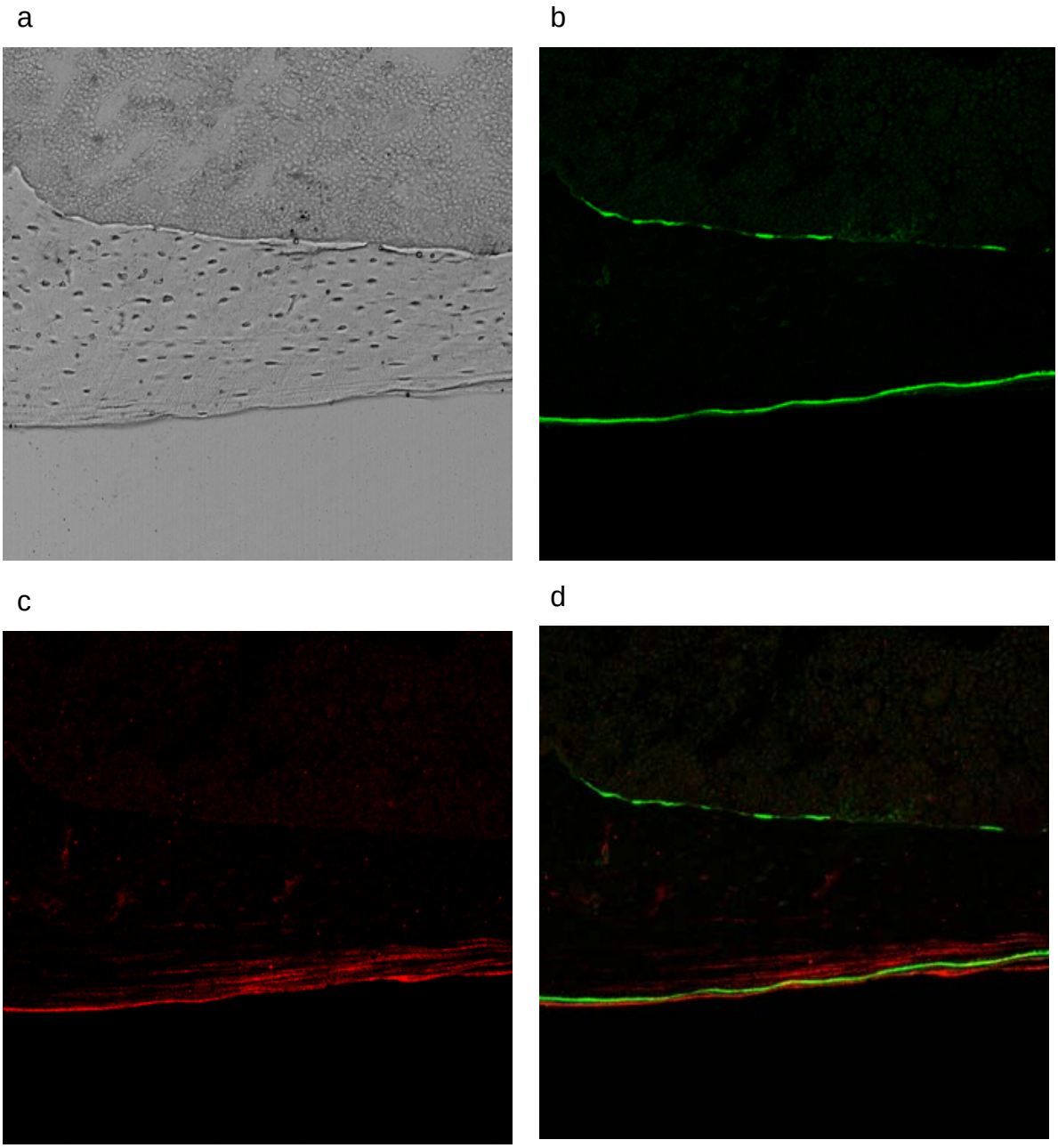

Figure S3. Organization of collagen fibers within the zone of periosteal bone mineralization in lean animals treated with SR10171 and visualized by Leica SPS Laser Scanning Confocal Multiphoton Microscope. (a) – bright light image of a cortical bone section at tibia midshaft; (b) – periosteal bone mineralization zone (green); (c) – collagen fibers (red); (d) – colocalization of the mineralization zone and collagen fibers.

Figure S4. Related to Figure 3.

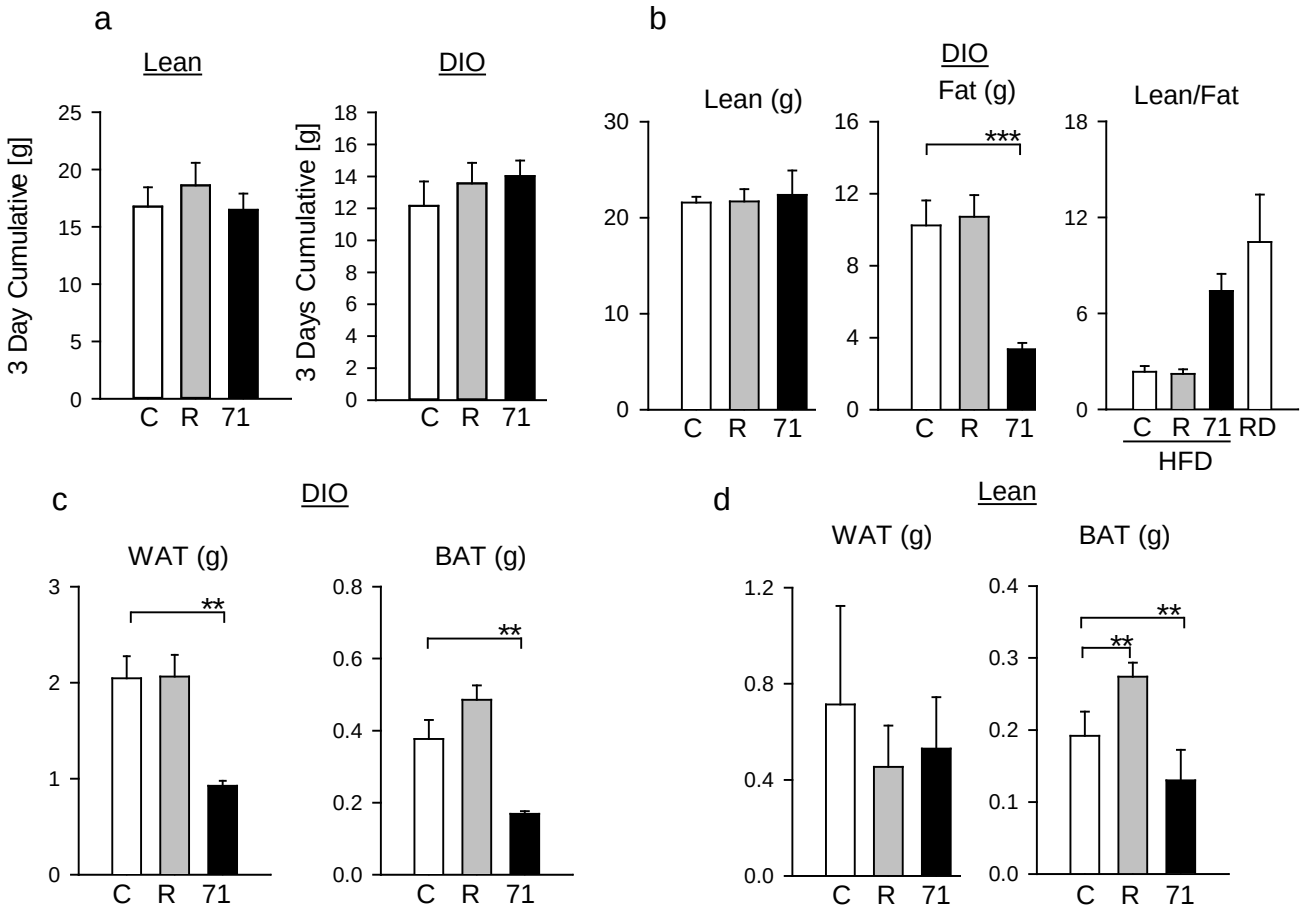

Figure S4. Effect of SR10171 and rosiglitazone on food consumption, and body composition. (a) Cumulative food consumption during a period of 3 days metabolic cages measurements of lean and DIO animals. (b) Body composition of DIO mice assessed by NMR. (c) Weights of epididymal, representing white adipose tissue (WAT), and interscapular, representing brown adipose tissue (BAT), of DIO mice. (d) Weights of WAT and BAT fat depots in lean animals. All measurements in (b), (c), and (d) were done at the end of experiment on all animals. Data are shown as the mean +/- SD. Statistical analyses were performed using One Way Anova and significant differences are shown between treated groups and control group. *P < 0.05; **P < 0.01; ***P < 0.001

Figure S5. related to Figure 4.

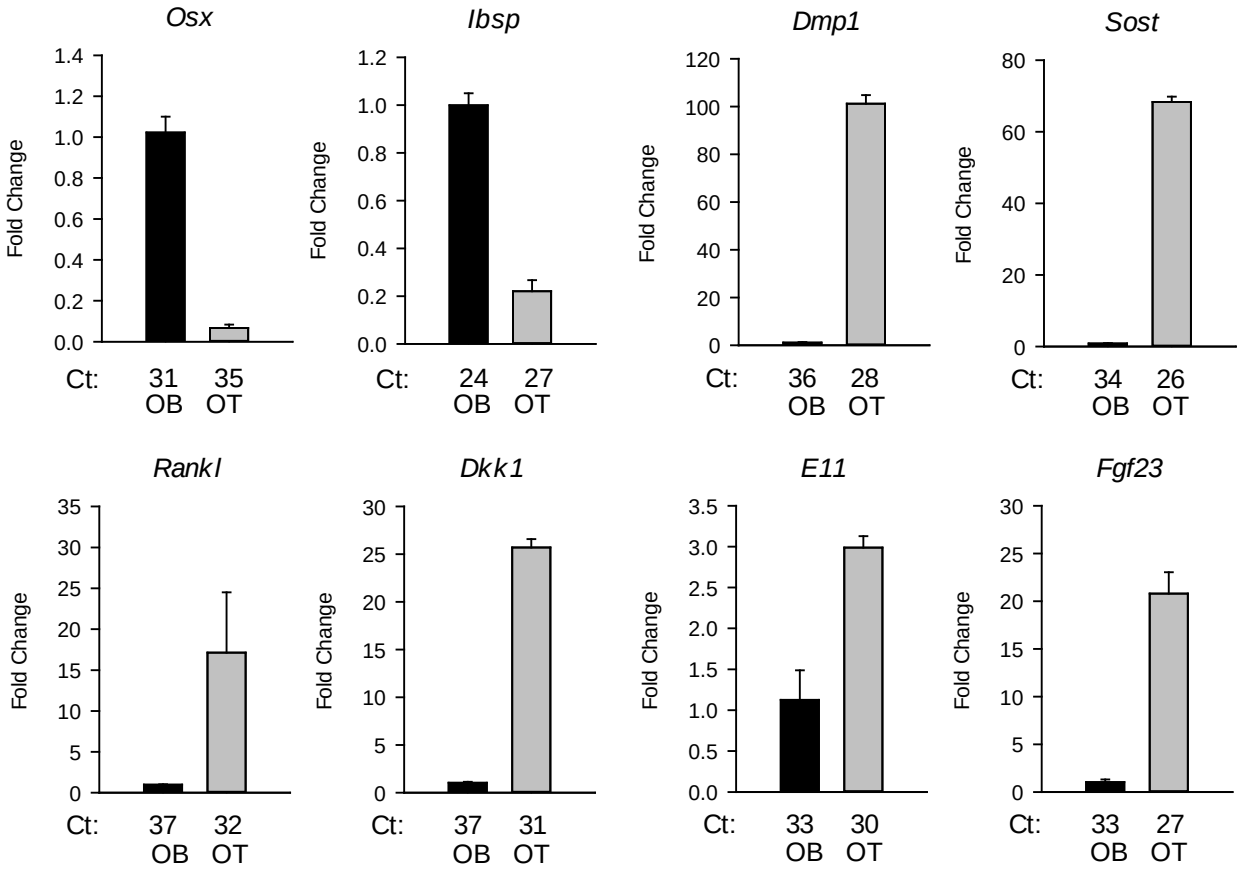

Figure S5. Comparison of osteoblast (OB) and osteocyte (OT) fractions isolated from femora of control lean animals for expression levels of osteoblast- and osteocyte-specific gene markers. Ct values indicate the cycle number at which specific RNA was detected.

Figure S6. Related to Figure 4.

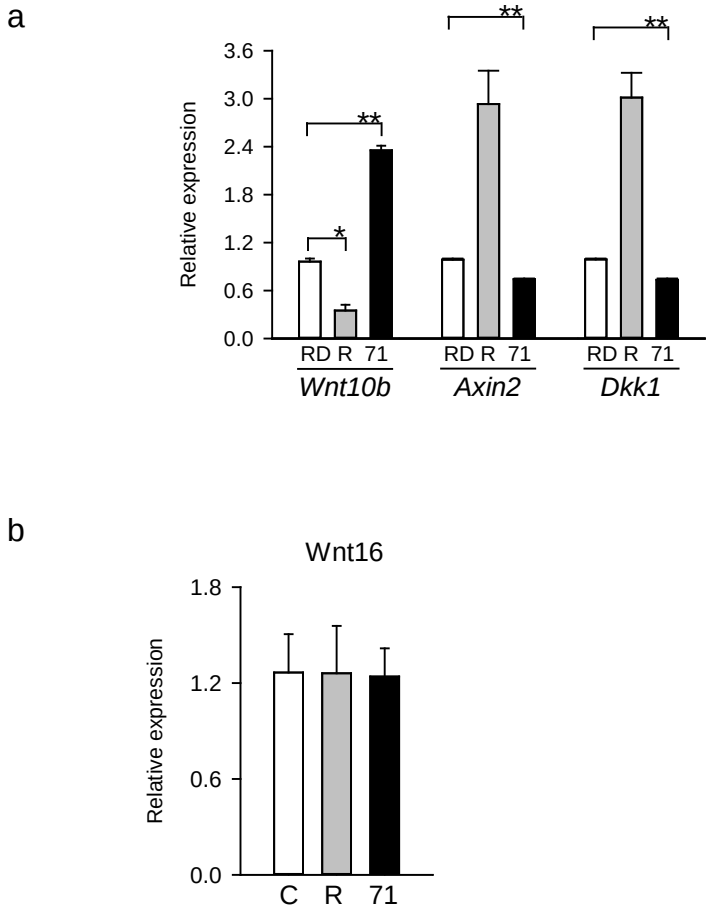

Figure S6. Analysis of gene expression of Wnt pathway signaling members. (a) Primary marrow MSCs treated *ex vivo* with 10 μM SR10171 or 1 μM rosiglitazone for 3 days. (b) Expression of Wnt16 in osteocytes freshly isolated from femora of treated animals. Data are shown as the mean +/- s.d. Statistical analyses were performed using One Way Anova and significant differences are shown between treated groups and control group. *P < 0.05; **P < 0.01

Table S1. Correlation between trabecular bone and marrow fat volume and bone loss or gain in DIO animals

Skeletal site	Treatment groups	Tissue volume (TV) (mm^3)	Bone volume (BV) (mm^3)	Fat volume (FV) (mm^3)	BV/TV (%)	FV/TV (%)	Bone volume gain or loss vs. control
L4 Vertebra	Control	2.663 ± 0.212	0.274 ± 0.038	0.002 ± 0.001	10.3 ± 1.3	0.08 ± 0.05	
	SR10171	2.787 ± 0.176	0.314 ± 0.103	0	11.1 ± 2.8	0	0
	Rosiglitazone	2.675 ± 0.411	0.182 ± 0.045*	1.192 ± 0.002***	6.7 ± 1.4*	44.5 ± 0.24*	-33%
Proximal Tibia	Control	3.297 ± 0.270	0.458 ± 0.059	0.012 ± 0.004	13.9 ± 0.9	0.33 ± 0.09	
	SR10171	4.057 ± 0.312*	0.598 ± 0.088*	0.004 ± 0.002*	14.7 ± 1.0	0.10 ± 0.06*	30.6%
	Rosiglitazone	3.515 ± 0.166	0.332 ± 0.046*	0.944 ± 0.276**	9.5 ± 1.3**	26.9 ± 7.97**	-27.5%

* $p < 0.05$ vs. control; ** $p < 0.01$ vs control; *** $p < 0.001$ vs. control

Table S2. Calorimetric measurements of respiratory parameters in DIO and lean mice at the end of treatment (values represent average of measurements repeated every 20 min for 72 hrs)

		VO2 (ml/hr/kg)	VCO2 (ml/hr/kg)	RER	Heat (kcal/hr/kg)	Locomotion (counts/20 min)
DIO	HF	4994.9±446.9	4056.9±389.3	0.8104±0.0109	100.6±9.1	335.7±222.6
	Rosi	5124.6±431.4	4202.7±409.9	0.8168±0.0156[a]	103.5±8.9	377.4±227.6
	171	5550.7±543.1[a,b]	4554.6±422.1[a,b]	0.8225±0.0137[a]	112.1±10.8[a,b]	481.6±269.1[d]
Lean	RD	4468.4±311.4[c]	4362.2±350.2[c]	0.9765±0.0160[c]	93.8±6.8[c]	828.9±433.1[c]
	Rosi	4533.7±309.8	4522.1±368.2	0.9949±0.0163[a]	95.7±6.8	762.1±351.5
	171	4391.9±356.7	4278.4±367.3[b]	0.9739±0.0151[b]	92.2±7.6[b]	1054.8±584.9[b]

HF – high fat diet control; RD – regular diet control; Rosi – rosiglitazone; 171 – SR10171

[a] $p<0.05$ vs. control; [b] $p<0.05$ vs. Rosi; [c] $p<0.05$ control HFD vs. control RD; [d] $p=0.066$

Table S3. Calculated statistical significance (p values) of respiratory parameters measurements listed in Table S2

		VO2	VCO2	RER	Heat	Locomotion
DIO	R vs HF	NS	NS	0.05	NS	NS
	71vs HF	0.00001	0.000002	0.00009	0.000007	0.01
	71vsR	0.004	0.0006	NS	0.004	NS
Lean	R vs RD	NS	0.07	0.000007	NS	NS
	71vs RD	NS	NS	NS	NS	NS
	71vs R	NS	0.006	0.0000003	0.04	0.01

HF – high fat diet control; RD – regular diet control; R – rosiglitazone; 71 – SR10171

NS – statistically nonsignificant, $p > 0.05$

Table S4. Primer sequences used for real-time PCR

Gene	F - Primer	R - Primer
18S	TTCGAACGTCTGCCCTATCAA	ATGGTAGGCACGGCGACTA
AdipoQ	GGCCGTTCTCTTCACCTACG	TGGAGGAGCACAGAGCCAG
FABP4	GCGTGGAATTCGATGAAATCA	CCCGCCATCTAGGGTTATGA
FoxC2	ACGAGTGCGGATTTGTAACC	ACAGTTGGGCAAGACGAAAC
Bmp4	TCAAGGGAGTGGAGATTGGG	GCCATCATGGCCAAAAGTG
Bmp2	AACTGGCTAGAATATTAAGCACTGCA	AGTGATTTCCTAACTGCCCAGG
Tbx1	GGCAGGCAGACGAATGTTC	TTGTCATCTACGGGCACAAAG
HoxC9	GCAGCAAGCACAAAGAGGAGAAG	GCGTCTGGTACTTGGTGTAGGG
Ucp1	GGATGGTGAACCCGACAACT	AACTCCGGCTGAGAAGATCTTG
Runx2	GGGCACAAGTTCTATCTGGAAAA	CGGTGTCACTGCGCTGAA
Osterix	AGTTCACCTGCCTGCTCTGT	GGAGCTGGAGACCTTCCTCT
Osteocalcin	CGGCCCTGAGTCTGACAAA	GCCGGAGTCTGTTCACTACCTT
Collagen I	ACTGTCCCAACCCCCAAAG	CGTATTCTTCCGGGCAGAAA
c-fos	AAGTATGCCCACACCAACTGATC	GAAAGCCCGTTCCCAAGAAA
Ctsk	AGCAGGCTGGAGGACTAAGGT	GATTTGTGCATCTCAGTGGAAGAC
Mepe	GAGAAGACCCAATTCCCACA	AACTCCCACTGGATGACGAC
Wnt10b	AATGAAGGTGAGCCTCGCC	TGAAAGAGAGCAGCCCTCACA
Wnt16	GGAGCTGTGCAAGAGGAAAC	GAAGTGGTAGTGGCGACCAT
Axin2	TAGGCGGAATGAAGATGGAC	CTGGTCACCCAACAAGGAGT
Dkk1	GAGGGGAAATTGAGGAAAGC	ACGGAGCCTTCTTGTCCTTT
Sost	CCTCCTCCTGAGAACAACCA	ACATCTTTGGCGTCATAGGG
RankL	CCTGAGGCCCAGCCATTT	CTTGGCCCAGCCTCGAT
Dmp1	TGTCATTCTCCTTGTGTTCCTTTG	AGAGCTTTCAGATTCAGTATTGTGGTAT
E11	GTGACCCCAGGTACAGGAGA	AGAGGTGCCTTGCCAGTAGA
Fgf23	AGGGACCTGCCTTAGACTCC	CCGGATAGGCTCTAGCAGTG
Ibsp	GAAGCAGGTGCAGAAGGAAC	GAAACCCGTTCAGAAGGACA
OPG	CAAGACATTGACCTCTGTGAAAGC	CGTGCAGCGGCATCTCGGC

Supplemental Material and Methods

Analysis of S112 and S273 phosphorylation

AD2 cells representing marrow preadipocytes were pre-treated with vehicle, 1 μM rosiglitazone, or 5 μM SR10171 for 1h followed by treatment with 50 ng/ml TNF-α for 1h followed by isolation of proteins by incubating pelleted cells with whole cell extract buffer (20mM HEPES, 25% glycerol, 0.42M NaCl, 0.2mM EDTA, pH 7.4) supplemented with protease and phosphatase inhibitors for 30 min on ice as described(Choi et al., 2010). The samples were centrifuged at 100,000g for 5 min at 4°C. Protein samples were resolved by 10% SDS polyacrylamide gel electrophoresis and electrophoretically transferred to Immobilon-FL membranes. Membranes were blocked at room temperature for 1h in TBS [10 mM Tris-HCl (pH 7.4), 150 mM NaCl] containing 3% BSA plus phosphatase inhibitors. Incubation with primary antibody was done overnight at 4°C. After three washes in TBST (TBS plus 0.1% Tween 20), membranes were incubated with infrared anti-rabbit (LI-COR Biosciences Cat# 926-32213, RRID:AB_621848, green) or anti-mouse (LI-COR Biosciences Cat# 926-68072, RRID:AB_10953628, red) secondary antibodies at 1:15,000 dilution in TBS for 2 h at 4°C. Immunoreactivity was visualized and quantified by infrared scanning in the Odyssey system (, Lincoln, NE) and band density was quantified using Image J software. Antibody against PPARγ (Santa Cruz Biotechnology Cat# sc-7273, RRID:AB_628115) was obtained from Santa Cruz Biotechnologies, working dilution 1:1,000. Ser-112 Phospho-PPARγ2 (ab195925) antibody was purchased from Abcam (Abcam PLC, Cambridge, MA), working dilution 1:500. Ser-273 Phospho-PPARγ2 (bs-4888R) antibody was purchased from Bioss Inc. (Bioss, Inc., Woburn, MA), working dilution 1:500.

Cell culture

Primary bone marrow cultures (PBMC) were established from femur marrow aspirates and colony forming units (CFU) assays were performed as described (Lazarenko et al., 2007). MLO-A5 cells were cultured on collagen coated plates in MEM-α supplemented with 5% fetal bovine serum (FBS) and 5% calf serum, PBMC were grown in MEM-α supplemented with 15% FBS, AD2 and U33 cells were grown in MEM-α supplemented with 10% FBS, whereas U33/γ2 cells were grown in the same as U33 media supplemented with 0.5 mg/ml G418. For osteoblast differentiation and mineralization of extracellular matrix cells were grown in the medium supplemented with 0.2 mM ascorbic acid and 10 mM β-glycerophosphate for 9 days (U33) or 26 days (PBMC). RAW264.7 cells, a murine monocyte/macrophage cell line, were cultured in MEM-α supplemented with 10% FBS, and 50 μg/ml of RANKL and 50 μg/ml M-CSF.

Primary osteocytes for *ex vivo* experiment were represented by cell outgrows from bone pieces remaining after serial collagenase digestion procedure (Kramer et al., 2010). Cells were cultured on type-I rat tail collagen-coated six-well plates in MEM-α supplemented with 5% FBS and 5% calf serum. Cultures were maintained at 37°C and 5% CO2 in a humidified incubator for 4 days. After 4 days, medium and bone pieces were removed and remaining cells were treated with ligands for 6 days followed by RNA isolation.

Knockdown of PPARα and PPARγ in MLO-A5 cells was achieved by lentiviral infection with shRNA (GTAGAAGCCGTGCAAGAGATCACAGAGTA) specific to mouse PPARα, or shRNA (AACATTCAAGAGATTTCTCAGTCCATCGG) specific to mouse PPARγ, as previously described(Hinds et al., 2011). A control MLO-A5 knockdown cell line was made by lentiviral infection with commercially scrambled shRNA (Santa Cruz Biotechnologies, CA).

Overexpression of hPPARγ not mutated (WT), or harboring a mutation of serine 273 to alanine (S273A) or serine 112 to alanine (S112A) (Hinds et al., 2011) which prevent serine phosphorylation were achieved using pCMV plasmid constructs carrying cDNA coding for each form of hPPARγ.

Extraction of osteoblast- and osteocyte-enriched fractions

Cell fractions enriched in either osteoblasts or osteocytes were isolated by sequential collagenase digestion of fresh femora bone, according to previously described protocol (Kramer et al., 2010), and immediately lysed for analysis of gene expression. The enrichment of each fraction with a desired cell type was assessed by comparing levels of expression of genes known to be more abundantly expressed in either osteoblasts (*Osx* and *Ibsp*) or osteocytes (*Dmp1*, *Sost*, *Rankl*, *Dkk1*, *E11*, and *FGF23*).

Osteoclastogenesis assay

Primary bone marrow cells (PBMC) were harvested, as previously described (Lazarenko et al., 2007), and seeded at the density of $2.5\times10^5/cm^2$ in the presence of MEM-α (Invitrogen, Carlsbad, CA) supplemented with 15% FBS (Hyclone, Waltham, MA). Floating, non-adherent cells were harvested after 24 hr and seeded at the density of $2\times10^5/cm^2$ into 48-well plate with the medium supplemented with M-CSF (50ng/ml) and RANKL (50ng/ml) (R&D System, Minneapolis, MN). After 3 days of growth, medium was replaced with fresh medium containing M-CSF, RANKL, and one of the following DMSO, rosiglitazone (1 μM), or SR10171(10 μM) . After 6 days of growth, cultures were either stained for tartrate resistant acid phosphatase (TRAP) using the Leukocyte Acid Phosphatase (TRAP+) Kit (Sigma), or harvested with TRIzol reagent (Sigma-Aldrich, St. Louis, MO) for total RNA isolation. Cells positive for TRAP staining with 4 or more nuclei were counted as osteoclasts. Counting was done in quadruplets.

Gene expression analysis

Total RNA was isolated using TRIzol reagent (Sigma-Aldrich, St. Louis, MO). One μg of RNA was converted to cDNA using the Verso cDNA synthesis kit (Thermo Fisher Scientific, Waltham, MA). An amplification of the cDNA were performed by quantitative real-time PCR using TrueAmp SYBR Green qPCR SuperMix (Smart Bioscience, Maumee, OH) and StepOne Plus System (Applied Biosystems, Carlsbad, California). The thermocycling protocol consisted of a single 10 min step at 95°C, 40 cycles of 15 s at 95°C and 60 s at 60°C primer-specific temperature followed by a melting curve stage ranging from 60–95°C to allow for evaluation of the product specificity. Relative gene expression was measured by the comparative ΔΔCT method using *18S* RNA levels for normalization. Primers were designed using OligoPerfect Designer (Thermo Fisher Scientific, Waltham, MA) and their sequences are listed in the Table S4.

Measurement of mice metabolic parameters

Animals' fat and lean mass were evaluated at the beginning and at the end of experiment using a Minispec mq10 NMR analyzer (Bruker, Billerica, Massachusetts). Glucose tolerance (glucose tolerance test, GTT) was tested after ip injection of 2 g/kg glucose to animals fasted for 4 hrs. Blood glucose was measured using the AlphaTRAK system appropriate for mice (Abbott Laboratories, North Chicago, Illinois). For indirect calorimetry, mice were evaluated in metabolic cages (CLAMS; Columbus Instruments, Columbus, Ohio) with a free access to food and water (n=4 per group). Measurements of CO_2 production, O_2 consumption, RER, heat, and ambulatory counts by x-peak were determined for 3 consecutive days after 24 hr adaptation and normalized to lean body mass as described (Tschop et al., 2012).

Micro CT imaging of bone and marrow fat

mCT of the tibiae was performed using the μCT-35 system (Scanco Medical AG, Bruettisellen, Switzerland), as previously described(Liu et al., 2012). Briefly, scans were performed at 7 μm nominal resolution with the x-ray source operating at 70 kVp, and 113 μA settings. Scans of proximal tibia consisted of 300 slices starting at the growth plate and images of trabecular bone were segmented at 220 threshold value using per mille scale following manual contouring starting 10 slices below the growth plate and extending to the end of the image stack. Scans of cortical bone at tibia midshaft consisted of 55 slices. Images of cortical bone were contoured in the entire image stack and segmented at 260 threshold using per mille scale. The analyses of the trabecular bone microstructure and the cortical bone parameters were conducted using Evaluation Program V6.5-1 (Scanco Medical AG, Bruettisellen, Switzerland) and conformed to recommended guidelines (Bouxsein et al., 2010).

For lipid content evaluation, decalcified bone specimens were stained for 1h in solution containing 2% osmium tetroxide prepared in 0.1M sodium cacodylate buffer pH 7.4, according to the protocol(Liu et al., 2012). Staining was carried-out in an exhaust hood and away from light due to osmium tetroxide toxicity and light sensitivity. Images of lipid depositions were acquired at 70 kVp and 113 μA settings and 12 μm nominal resolution. Image segmentation was done under global threshold condition by applying a threshold of 480-1000 using permille scale with 3-dimensional noise filter set to sigma 1.2 and support 2.0. Lipid volumes were calculated directly from individual voxel volumes in 3-D reconstructions. All mCT measurements were performed in a blind fashion.

Bone histomorphometry

To obtain static and dynamic bone histomorphometry, animals were injected with 2.5 mg/ml calcein solution in 2% sodium bicarbonate at a dose 20 mg/kg body weight. First injection was performed 10 days and second 2 days before sacrifice. Undecalcified tibiae were embedded in methyl methacrylate, sectioned and stained with either Golden

Trichrome or Von Kossa/McNeal by Histology Core at the Department of Anatomy and Cell Biology, Indiana University (Indianapolis, IN). The histomorphometric examination was confined to the secondary spongiosa of proximal tibia and was performed using Nikon NIS-Elements BR3.1 system. The measurements were collected under 20× and 40× magnification from six representative fields per bone sample. The histomorphometric examination of the cortical bone was confined to the periosteal surface of the midshaft tibia and was performed using Nikon NIS-Elements BR3.1 system. The measurements were collected under 5× magnification from a representative field per bone sample. Lacunae density was calculated by using the automated counter from the Nikon NIS-Elements BR3.1 system and dividing the total number by the area of bone.

The terminology and units used were those recommended by the Histomorphometry Nomenclature Committee of the American Society for Bone and Mineral Research (Parfitt et al., 1987). All histomorphometry analyzes were performed in a blind fashion.

LanthaScreen TR-FRET Competitive Binding Assay for PPARγ PPARγ competitive binding assay (Invitrogen, Carslbad, CA) was performed according to the manufacturer's protocol. A mixture of 0.5 nM glutathione S-transferase fused with human PPARγ ligand binding domain (GST–PPARγ– LBD), 5 nM Tb-GST-antibody, 5 nM Fluormone Pan-PPAR Green, and serial dilutions of compound beginning at 10 μM downwards was added to wells of black 384-well low-volume plates (Greiner Bio One, Monroe, NC) to a total volume of 18 μL, with all wells containing 2% DMSO. All dilutions were made in TR-FRET PPAR assay buffer. Experiments were performed in triplicates and incubated for 2 h in the dark before analysis in Perkin Elmer ViewLux ultra HTS microplate reader (PerkinElmer, Waltham, MA). The FRET signal was measured by excitation at 340 nm and emission at 520 nm for fluorescein and 490 nm for terbium. Graphs were plotted using GraphPad Prism software (GraphPad, La Jolla, CA) and EC50 was calculated.

Hydrogen/deuterium exchange mass spectrometry (HDX-MS)

Full length PPARγ2 was expressed in *E.coli* BL21 (DE3) cells. Solution-phase amide HDX was performed with a fully automated system as described previously with minor modifications(Marciano et al., 2015). For differential HDX experiments, 5μL of a 10μM PPARγ2 solution (Apo or in complex with 10-excess compound SR10171 or SR2595 or rosiglitazone) was diluted to 25μL with D_2O-containing HDX buffer, and incubated at 4°C for; 10s, 30s, 60s, 900s, and 3,600s. Following on-exchange, unwanted forward or back exchange is minimized and the protein is denatured by dilution to 50μL with 0.1% TFA in 3M urea (held at 4° C, pH 2.5). Samples are then passed across an immobilized pepsin column (prepared in house) at 50μL min-1 (0.1% TFA,15°C) and the resulting peptides are trapped onto a C_8 trap cartridge (Thermo Fisher, Hypersil Gold). Peptides were then gradient eluted (4% CH_3CN to 40% CH_3CN, 0.3% formic acid over 5 minutes, 4°C) across a 1mm x 50mm C_{18} HPLC column (Hypersil Gold, Thermo Fisher) and electrosprayed directly into a high resolution orbitrap mass spectrometer (Exactive, Thermo Fisher). Percent deuterium exchange values for peptide isotopic envelopes at each time point were calculated and processed using HDX Workbench. HDX data is presented as an average of three individual replicates across 6 time points (10s, 60s, 300s, 900s, and 3,600s).

NR box peptide interaction assay

A TR-FRET-based interaction assay was used. The full length His-PPARγ2 and FITC-labeled peptides p300 (sequence: ASKHKQLSELLRSGSS), SMRT-2 (TNMGLEAIIRKALMGKYDQWEE), SRC1-2 (LTERHKILHRLLQEGSPSD), and NCOR1-3 (ASNLGLEDIIRKALMGSFD) were used. TR-FRET reaction contains 5nM PPARγ2, 450nM respective FITC peptide and compound (SR10171/SR2595/rosi) at various concentrations in assay buffer (TR-FRET Coregulator Buffer D, Lifetechnologies). The mixtures were incubated for 2hr at R.T., and fluorescence intensity was measured on an Envision pate reader with excitation at 340nm and emission at 490nm and 520 nm. The ratio of intensity at 520 nm/490nm was used to calculate cofactor recruitment activity.

***In Silico* Docking**

SR10171 and SR2595 were both docked into PPARγ using ICM Molsoft software which implements an algorithm of a biased probability Monte Carlo (BPMC) procedure (PMID: 8289329). In brief, chain A of PDB:4R06 (PMID: 26579553) was used as the receptor once waters were deleted, hydrogen atoms were added, and charges added. Both compounds were docked and the lowest energy poses were used for interpretation. Figures were generated in PyMol (Schrodinger).

Supplemental References

Bouxsein, M.L., Boyd, S.K., Christiansen, B.A., Guldberg, R.E., Jepsen, K.J., and Muller, R. (2010). Guidelines for assessment of bone microstructure in rodents using micro-computed tomography. J Bone Miner Res *25*, 1468-1486.

Choi, J.H., Banks, A.S., Estall, J.L., Kajimura, S., Bostrom, P., Laznik, D., Ruas, J.L., Chalmers, M.J., Kamenecka, T.M., Bluher, M., et al. (2010). Anti-diabetic drugs inhibit obesity-linked phosphorylation of PPARgamma by Cdk5. Nature *466*, 451-456.

Hinds, T.D., Jr., Stechschulte, L.A., Cash, H.A., Whisler, D., Banerjee, A., Yong, W., Khuder, S.S., Kaw, M.K., Shou, W., Najjar, S.M., et al. (2011). Protein phosphatase 5 mediates lipid metabolism through reciprocal control of glucocorticoid and PPAR{gamma} receptors. J Biol Chem *286*, 42911-42922.

Kramer, I., Halleux, C., Keller, H., Pegurri, M., Gooi, J.H., Weber, P.B., Feng, J.Q., Bonewald, L.F., and Kneissel, M. (2010). Osteocyte Wnt/beta-catenin signaling is required for normal bone homeostasis. Mol Cell Biol *30*, 3071-3085.

Lazarenko, O.P., Rzonca, S.O., Hogue, W.R., Swain, F.L., Suva, L.J., and Lecka-Czernik, B. (2007). Rosiglitazone induces decreases in bone mass and strength that are reminiscent of aged bone. Endocrinology *148*, 2669-2680.

Liu, L., Aronson, J., Huang, S., Lu, Y., Czernik, P., Rahman, S., Kolli, V., Suva, L.J., and Lecka-Czernik, B. (2012). Rosiglitazone inhibits bone regeneration and causes significant accumulation of fat at sites of new bone formation. Calcif Tissue Int *91*, 139-148.

Marciano, D.P., Kuruvilla, D.S., Boregowda, S.V., Asteian, A., Hughes, T.S., Garcia-Ordonez, R., Corzo, C.A., Khan, T.M., Novick, S.J., Park, H., et al. (2015). Pharmacological repression of PPARgamma promotes osteogenesis. Nature communications *6*, 7443.

Parfitt, A.M., Drezner, M.K., Glorieux, F.H., Kanis, J.A., Malluche, H., Meunier, P.J., Ott, S.M., and Recker, R.R. (1987). Bone histomorphometry: standardization of nomenclature, symbols, and units. Report of the ASBMR Histomorphometry Nomenclature Committee. J Bone Miner Res *2*, 595-610.

Tschop, M.H., Speakman, J.R., Arch, J.R., Auwerx, J., Bruning, J.C., Chan, L., Eckel, R.H., Farese, R.V., Jr., Galgani, J.E., Hambly, C., et al. (2012). A guide to analysis of mouse energy metabolism. Nat Methods *9*, 57-63.